Assessing Entropy and Fractal Dimensions as Discriminants of Seizures in EEG Time Series

Ahmed El-Kishky
Tandy School of Computer Science
The University of Tulsa
Tulsa, Oklahoma 74104-9700
Email: ahmed-el-kishky@utulsa.edu

Abstract—**In this paper, the performance of Higuichi's algorithm for calculation of fractal dimension, Hurst exponents, and Shannon Entropy as discriminants for the detection of epileptic seizures in EEG signals are assessed. The proposed methods were applied to intracranial EEG recordings from epilepsy patients during the seizure free interval from within and from outside the seizure generating area as well as intracranial EEG recordings during epileptic seizures. Analysis was conducted using statistical hypothesis testing to determine the validity of the proposed seizure-identifying techniques.**

I. Introduction

The National Institutes of Health defines epilepsy as a brain disorder in which a person has repeated seizures (convulsions) over time. These seizures are further defined as episodes of disturbed brain activity that cause changes in attention or behavior. Standard diagnostic of epilepsy involves the manual analysis of Electroencephalogram (EEG) recordings. With inspection and identification of changes in the normal pattern of the brain's electrical activity, seizures can be identified.

The common diagnostic of epilepsy through visual scanning of EEG recordings for disturbances and spikes indicating seizures is a time-consuming process. Often EEG recordings may be quite long and visual diagnosis is very subjective.

Fractal dimension are considered an important parameter and feature of EEG signals and biosignals in general. These features have been studied on various EEG time signals and have often been applied to the study of epilepsy on EEG [1,2]. Intimately related to fractal dimensions, the Hurst exponent has been used as feature extraction of epileptic EEG [3]. The concept of entropy has been been used in the study of the complexity and characteristics of seizure onset [4].

These three metrics have been proposed to automate and standardize the process of seizure identification within EEG signals. Through the reduction short-length EEG time series into a single descriptive numerical value through means of Higuchi's algorithm for fractal dimensions, approximations of the generalized Hurst Exponent, and calculation of Shannon Entropy, distinctions between seizure-free intervals and seizure-containing intervals can theoretically be used to detect seizures within time series. For each method proposed, the polarization of the feature between seizure-containing and seizure free is assessed providing a metric for the feature as a discriminant.

II. Data Sets and Acquisition

EEG recordings for analysis were obtained from the Department of Epileptology at the University of Bonn [5]. Three data sets were used in this study each containing 100 23.6-sec EEG segments. The data sets originated from an EEG archive of pre-surgical diagnosis of epilepsy. Segments in Set A consisted of data from five patients and were obtained intracranially from the hippocampal formation of the brain. Segments in Set B consisted of data from five patients and were obtained from the hippocampal formation in the opposite hemisphere of the brain; the portion identified post resection as the epileptogenic zone. Both sets A and B consisted of data depicting brain activity during seizure-free intervals. Set C consisted of segments recorded intracranially of exclusively seizure activity.

The EEG signals were recorded with the same 128- channel amplifier system, after analog to digital conversion of the signal, the data was written to disk at a sampling rate of 173.61 Hz. The bandwidth of the acquisition system was 0.5 Hz to 85 Hz.

III. Methods of Analysis

Seizure Detection Metrics: Several measures for the detection of seizures within EEG time series have been proposed and will be discussed in this section. The results will be discussed in the next section.

A. Denoising

As information of interest lay below 40 Hz, and the time series possessed the spectral bandwidth of the acquisition system, a fifth-order Butterworth low pass filter was applied to each sample to denoise the digital signal [6,10]. The resulting time series possessed a bandwidth of 0.5 Hz to 40 Hz.

B. Fractal Dimension

The idea of fractals was first introduced by Benoit Mandelbrot in 1970s. A fractal is a geometric shape with the property of self-similarity. An object with D-dimensions when reduced by a factor of $\frac{1}{x}$ in each of its spatial directions requires $N = x^D$ self-similar copies to cover the original object. An example is the euclidean forms of a line, square, and cube with one, two, and three dimension respectively. With $x = 2$, a line needs 2^1 lines of $\frac{1}{2}$ the original size to fill the original

978-1-4673-0382-8/12/$31.00 ©2012 IEEE

Fig. 1. Sample Denoised Time Series

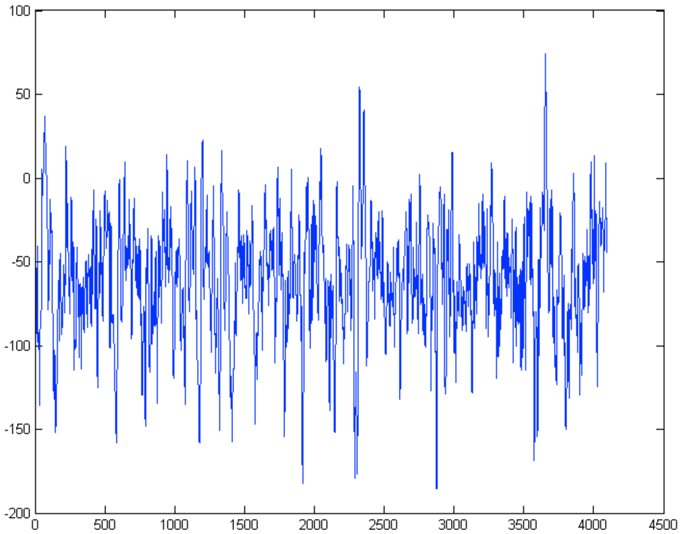

line, for a square 2^2 squares with each side half the length of the original square, and for the cube 2^3 cubes each with sides half the length of the side of the original cube. The dimension D of a shape is expressed as

$$D = \lim_{x\to+0} \frac{ln(N(x))}{ln(x)}.$$

Thus the fractal dimension is calculated as the tangent of $ln(x)$ vs $ln(N)$.

Fractal dimensions can be used to measure the amount of chaos in a time series and thus provide a possible metric for the detection of certain disturbances from the norm within brain activity. To calculate the fractal dimension D_f of each time series segment, Higuchi's algorithm was used [7,8]. Higuchi's algorithm is specifically designed for approximating the fractal dimension of time series data. Higuchi's algorithm creates k new time series. If the original time series takes the form

$$x = \{x(0), x(1), \ldots x(N)\}$$

Each constructed time series possesses k points and takes the form

$$y_m = \{x(m), x(m+k), x(m+2k), \ldots x(\lfloor \frac{N-m}{k} \rfloor)\}.$$

For each time series constructed, the average length $L(k)$ of each curve is computed and plotted against its corresponding k value on a log-log scale. The length, $L_m(k)$ of each curve X_m^k is represented by

$$L_m(k) = \frac{1}{k}|(\sum_{i=1}^{M} |X(m+i*k) - X(m+(i-1)*k)|)| \frac{N-1}{M*k}$$

As $L_m(k)$ represents the sum of absolute values of difference in ordinates of pair of points distant k after normalization, it is not truly the length. The length of curve for the time interval k, is the mean of the k values $L_m(k)$ for $m = 1, 2, \ldots k$. The slope of the resultant linear regression provides an estimate of the fractal dimension. As Higuchi's algorithm requires the selection of a k_{max}, this was selected by plotting D_f vs k_{max} and identifying the k_{max} at which the D_f plateau [9]. A k_{max} value of 30 was selected. Fractal dimensions for each segment in sets A, B, and C were computed.

C. Generalized Hurst Exponent

The Hurst exponent is a numerical estimate of the predictability of a time series [11-13]. It is defined as the relative tendency of a time series to either regress to a longer term mean value or 'cluster' in a direction. The underlying assumption of the dataset is that the time series approximates a fractal – as such the hurst exponent is an estimate. Values of the Hurst exponent range from 0 to 1. A hurst exponent $h \in [0, 0.5)$ indicates anti-persistent data. An increase is likely to be followed by a decrease and a decrease likely to be followed by an increase. ($i.e.$ $x[t-1] > x[t]$ $predicts$ $x[t] < x[t+1]$). This switching from from increasing to decreasing and vice versa is likely to persist in the time series over time with the strength increasing as $h \to 0$. $h \in (0.5, 1]$ indicates persistence within the time series. Such an h value implies that increasing tendencies will probably persist and decreasing tendencies will probably persist ($i.e.$ $x[t-1] < x[t]$ $predicts$ $x[t] < x[t+1]$). The strength of this trend increases as $h \to 1$. $h = 0.5$ implies that there is likely no correlation between an element and a future element.

As the Hurst exponent can classify time series based on their predictability and chaos levels, it may be a useful tool in identifying deviations from the normal patters of brain activity during interruptions of seizures [14]. The Hurst exponent was calculated for each segment within data sets A, B, C.

D. Shannon Entropy

In information theory and communication, entropy is considered the amount of uncertainty within a random variable. If the entropy is 0, that indicates that the system is predictable. Due to the chaotic nature of seizure in relation to non-seizure activity, the Shannon entropy of time series was proposed as a metric of seizure detection. In the following expressions, s is the signal and s_i the coefficients of s in an orthonormal basis. Entropy E is an additive cost function with the following properties [15,16].

$$E(0) = 0 \text{ and } E(s) = \sum_{i=0}^{n} E(s_i)$$

Therefore the nonnormalized Shannon Entropy is

$$E(s_i) = s_i^2 log(s_i)^2$$

$$E(s) = -\sum_{i=0}^{n} s_i^2 log(s_i)^2$$

The Shannon entropy in each segment within data sets A, B, C were calculated.

IV. Results and Discussion

For comparisons of the validity of each algorithm as a possible metric for the detection of seizures, statistical measures of the values obtained from each algorithm were analyzed and two-sample Student's t-test were calculated at the 5% significance level.

A. Higuchi's Algorithm for Fractal Dimensions

Higuchi's algorithm showed promise in differentiating between EEG segments with seizures and seizure-free EEG segments. $Figure$ 2 displays a plot of fractal dimension calculated in seizure free intervals in the hippocampal regions of the brain. There seems to be no differentiation between the fractal dimension from epileptogenic samples in Set B and those of the opposite hemisphere in Set A. As seen in $Figure$ 3 and $Figure$ 4, in differentiating between seizure free intervals and seizure-containing intervals, the fractal dimension of the time series for both Set A and Set B showed delineation with seizure-free intervals possessing a lower fractal dimension than intervals containing seizures of Set C. Student's two-sample t-test were run between the fractal dimension of Set A and Set B with the null hypothesis of both samples coming from the same population, and the result was a failure to reject the hypothesis. In the case of two-sample independent t-test run with both Set A and Set C as well as Set B and Set C, the null hypothesis was rejected at the 5% significance level. There did not exist sufficient statistical evidence to suggest that the fractal dimensions of seizure-free intervals could not be distinguished from seizure-containing intervals. Statistical data can be seen below.

Fractal Dimension			
Set	Size	Mean	Std. Dev.
A	100	1.4893	0.0821
B	100	1.4915	0.0978
C	100	1.6567	0.1226

B. Generalized Hurst Exponent

The generalized Hurst exponent did not provide a clear differentiation between seizure-free segments in EEG recordings from seizure-containing segments in visualization. Visualization shows no significant differences among the distribution of generalized Hurst Exponents for seizure-free time series and seizure-containing time series. Observing statistical data, the generalized Hurst exponent between the epileptogenic region and the non epileptogenic regions possessed means of approximately equal value. In addition these values were of higher than 0.5 indicating a stronger persistence. The generalized Hurst Exponent of Set C was lower than that of Sets A and B approaching 0.5 indicating a weaker trend in persistence and more uncertainty. Student's two-sample t-test were run between the generalized Hurst Exponents of Set A and Set B with the null hypothesis of both samples coming from the same population, and the result was a rejection of the hypothesis. In the case of two-sample independent t-test run with both Set A and Set C as well as Set B and Set C, the null hypothesis was rejected at the 5% significance level. There did not exist sufficient statistical evidence to suggest that the generalized Hurst Exponent of seizure-free intervals could not be distinguished from seizure-containing intervals. As $|0.5 - \mu_C| < |0.5 - \mu_A|$ and $|0.5 - \mu_C| < |0.5 - \mu_B|$, seizure-containing time series are likely to be more uncorrelated than seizure-free time series. Statistical data can be seen below.

Generalized Hurst Exponent			
Set	Size	Mean	Std. Dev.
A	100	0.7119	0.0733
B	100	0.7328	0.0607
C	100	0.6573	0.1027

C. Shannon Entropy

The Shannon Entropy of the time series provided a clear delineation between seizure-free segments and seizure-containing segments both visually and through statistical testing. Visualization of the Shannon Entropy of Sets A and B does not provide much delineation between the recordings obtained in seizure-free intervals. Yet, as seen in $Figure$ 8, the visualization of the entropies of Sets A and B with respect to the entropy of Set C, showed a distinct trend of the Shannon Entropy of seizure-containing segments to possess a higher magnitude of entropy than seizure-free intervals. This is demonstrated by the more negative values of the entropies of Set C in relation to Sets A and B; this is seen in $Figures$ 9 and 10. Student's two-sample t-test were run between the Shannon Entropies of Set A and Set B with the null hypothesis stating both samples were obtained from the same population, and the result was a failure to reject the null hypothesis. In the case of two-sample independent t-test run with both Set A and Set C as well as Set B and Set C, the null hypothesis was rejected at the 5% significance level. There did not exist sufficient statistical evidence to suggest that the Shannon Entropy of seizure-free intervals can not be distinguished from seizure-containing intervals. The mean of the entropy of Set C appears to be a of a magnitude of approximately $10\times$ that of the entropies of Sets A and B. In addition the Shannon Entropy of seizure-free recordings from the recognized epileptogenic zone on occasion seemed to possess similar qualities to entropies obtained during seizures.

Shannon Entropy			
Set	Size	Mean	Std. Dev.
A	100	-5.0565×10^7	5.7227×10^7
B	100	-2.3177×10^8	9.9224×10^8
C	100	-2.7503×10^9	2.5398×10^9

Fig. 2. Higuchi's Algorithm: A vs B

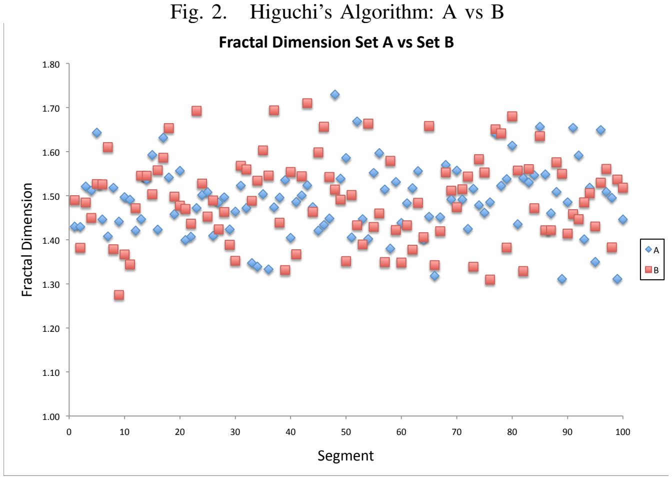

Fig. 5. Generalized Hurst Exponent: A vs B

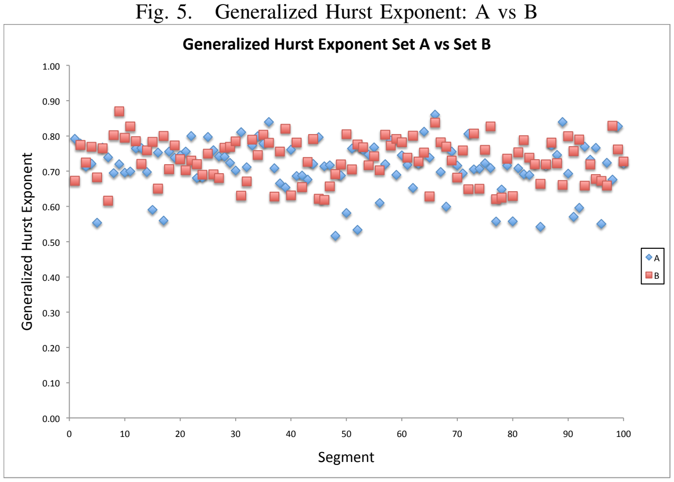

Fig. 3. Higuchi's Algorithm: A vs C

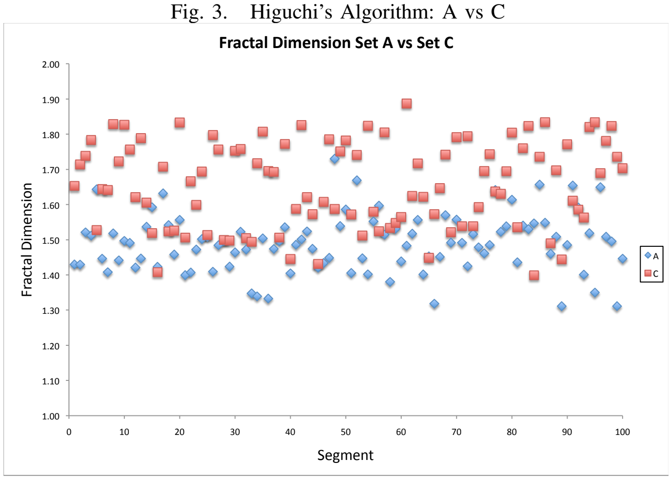

Fig. 6. Generalized Hurst Exponent: A vs C

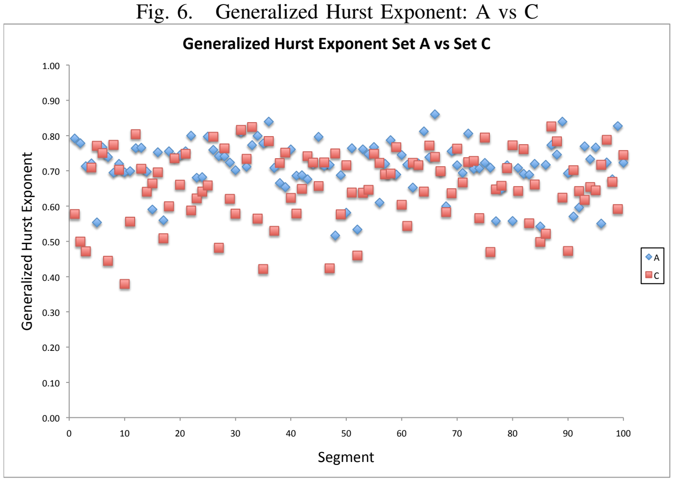

Fig. 4. Higuchi's Algorithm: B vs C

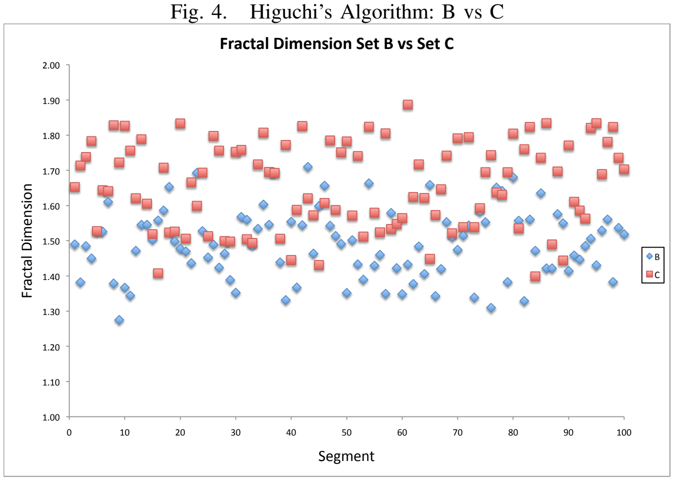

Fig. 7. Generalized Hurst Exponent: B vs C

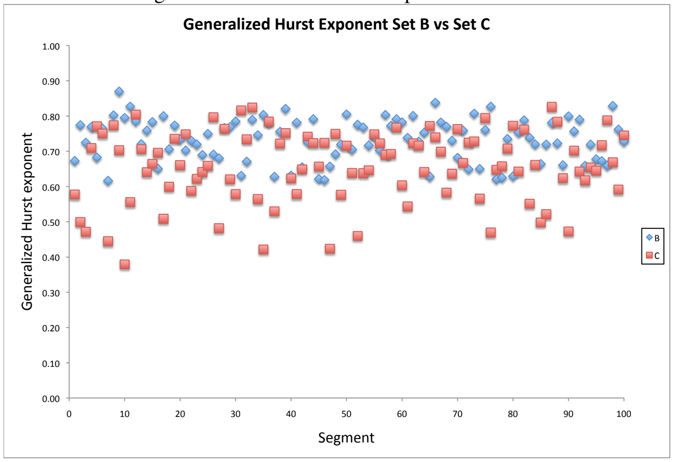

Fig. 8. Shannon Entropy: A vs B

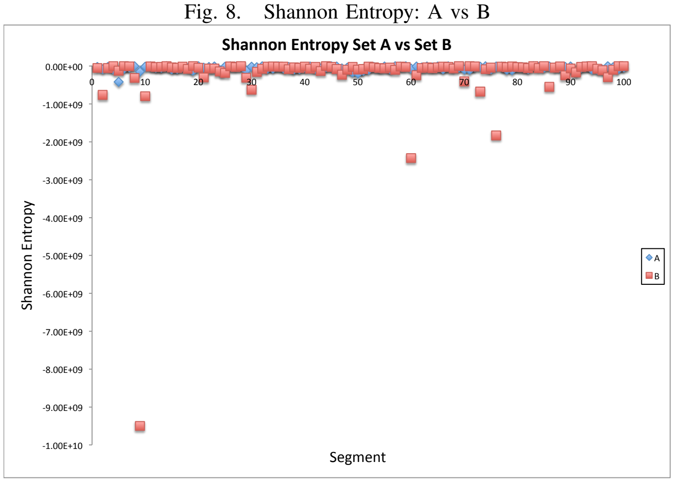

Fig. 9. Shannon Entropy: A vs C

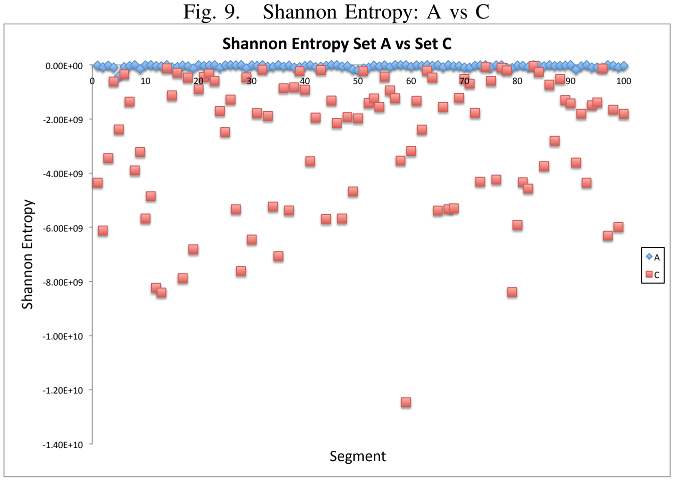

Fig. 10. Shannon Entropy: B vs C

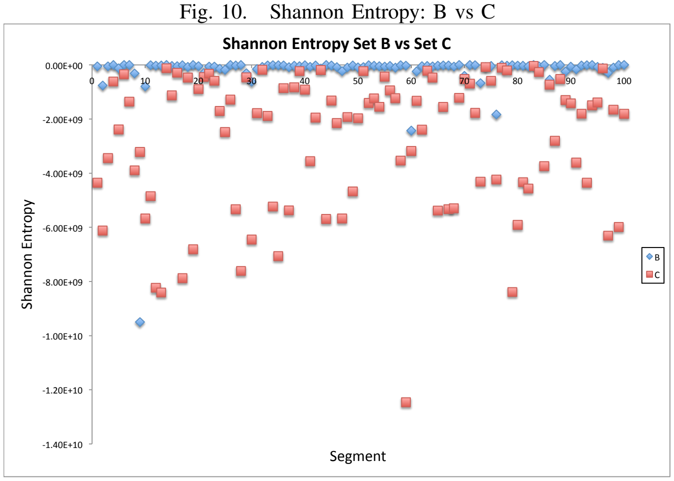

V. Conclusion

In this paper, three metrics were assessed in their effectiveness in detection of seizure in EEG signals. Of the three metrics, all three provided statistical differentiation between seizure-free recording and seizure containing time series.

Shannon entropy provided the strongest differentiation between seizure-free intervals and seizure containing intervals. In addition, Shannon Entropy in sporadic cases showed similarity in values between seizure-containing intervals and seizure-free intervals found in the verified epileptogenic hippocampal region. These values were not located in data obtained from the hippocampal region in the opposite region of the brain. This could provide a diagnostic for determining and isolating the epileptogenic zone of individuals with epilepsy.

As this study verified the existence of statistically significant differences between certain features of EEG time series containing seizures to those seizure-free, further study should attempt to verify this difference on out-of-sample data sets. Following verification on multiple data sets, machine learning algorithms such as artificial neural networks, decision trees, and other classifiers can utilize the three features as attributes in the detection of seizures within time series.

References

[1] Truong Quang Dang Khoa, Vo Quang Ha, and Vo Van Toi, Higuchi Fractal Properties of Onset Epilepsy Electroencephalogram, Computational and Mathematical Methods in Medicine, vol. 2012.

[2] E.T. Bullmore, M.J. Brammer, P. Bourlon, G. Alarcon, C.E. Polkey, R. Elwes, C.D. Binnie, Fractal analysis of electroencephalographic signals intracerebrally recorded during 35 epileptic seizures: evaluation of a new method for synoptic visualisation of ictal events, Electroencephalography and Clinical Neurophysiology, Volume 91, Issue 5, November 1994, Pages 337-345.

[3] EEG non-linear feature extraction using correlation dimension and Hurst exponent. Geng S, Zhou W, Yuan Q, Cai D, Zeng Y. Neurol Res. 2011 Nov;33(9):908-12.

[4] Characterization of early partial seizure onset: frequency, complexity and entropy. Jouny CC, Bergey GK. Clin Neurophysiol. 2012 Apr;123(4):658-69. Epub 2011 Aug 26.

[5] EEG time series are available under http://www.meb.uni-bonn.de/epileptologie/science/physik/eegdata.html

[6] Andrzejak RG, Lehnertz K, Rieke C, Mormann F, David P, Elger CE (2001) Indications of nonlinear deterministic and finite dimensional structures in time series of brain electrical activity: Dependence on recording region and brain state, Phys. Rev. E, 64, 061907

[7] Higuchi T. (1988). Approach to an Irregular Time Series on the Basis of the Fractal Theory, Physica D: Nonlinear Phenomena, 31, 277-283.

[8] Georgiev, S., Minchev, Z., Christova, C., & Philipova, D. (2009). EEG Fractal Dimension Measurement before and after Human Auditory Stimulation. Retrieved from http://cogprints.org/6757/

[9] Doyle TL, Dugan EL, Humphries B, Newton RU. Discriminating between elderly and young using a fractal dimension analysis of centre of pressure. Int J Med Sci. 2004;1:1120.

[10] M. Teplan. Fundamentals of EEG measurement. Measurement Science Review, 2:111, 2002.

[11] T. Di Matteo, T. Aste and M. M. Dacorogna, "Scaling behaviors in differently developed markets", Physica A 324 (2003) 183-188.

[12] T. Di Matteo, T. Aste and M. M. Dacorogna, "Long term memories of developed and emerging markets: using the scaling analysis to characterize their stage of development", Journal of Banking & Finance 29/4 (2005) 827-851.

[13] R. Acharya, O. Faust, N. Kannathal, et al., Non-linear analysis of EEG signals at various sleep stages, Comput. Meth. Programs Biomed. 80 (2005) 40–41.

[14] DePetrillo P.B., Speers D., Ruttimann U.E. Determining the Hurst exponent of fractal time series and its application to electrocardiographic analysis. Comp. Biol. Med. (1999).

[15] Coifman, R.R.; M.V. Wickerhauser (1992), "Entropy-based Algorithms for best basis selection," IEEE Trans. on Inf. Theory, vol. 38, 2, pp. 713–718.

[16] Donoho, D.L.; I.M. Johnstone, "Ideal de-noising in an orthonormal basis chosen from a library of bases," C.R.A.S. Paris, Ser. I, t. 319, pp. 1317–1322.